Spatial and temporal analysis of *Phytophthora megakarya* epidemic in newly established cacao plantations

Ndoungué Djeumekop M. M.[1,2,A] , Ngo Bieng M. A[3], Ribeyre F.[4], Bonnot F[5]., Cilas C[4], Neema C[2] and Ten Hoopen G. M.[1,6]

[1] IRAD, Laboratoire de Phytopathologie, BP 2123 Yaoundé, Cameroun

[2] Montpellier SupAgro, UMR BGPI, F-34398 Montpellier, France

[3] CIRAD, UPR Forêts et Sociétés, CATIE, Costa Rica. Forêts et Sociétés, Univ Montpellier, CIRAD, Montpellier, France.

[4] CIRAD, UPR Bioagresseurs, F-34398 Montpellier, France. Bioagresseurs, Univ Montpellier, CIRAD, Montpellier, France.

[5] CIRAD, UMR BGPI, F-34398 Montpellier, France. BGPI, Univ Montpellier, CIRAD, Montpellier, France.

[6] CIRAD, UPR Bioagresseurs, Cocoa Research Centre, Trinidad and Tobago. Bioagresseurs, Univ Montpellier, CIRAD, Montpellier, France.

[A] Author for correspondence:

Tel: (+237) 694025128

Email: mireillendoung2015@yahoo.fr

Abstract

Studying spatial and temporal plant disease dynamics helps to understand pathogen dispersal processes and improve disease control recommendations. In this study, three cacao plots devoid of primary inoculum of *Phytophthora megakarya* (causal agent of cacao black pod rot disease) upon establishment in 2006 were monitored for presence of disease on a weekly basis from 2009 to 2016. Ripley's K(r) function, join count statistics and Fisher Exact test were used to analyse spatial and temporal disease dynamics. Disease distribution maps showed aggregated disease patterns in all plots although for the years of disease onset, exogenous primary infections were mostly randomly distributed. The K(r) function confirmed these results indicating that inoculum generally disperses only over short distances. Moreover, significant positive spatial autocorrelations showed that diseased trees were often clustered up to a distance of 3-9 m. Temporal disease progression was low, meaning that endogenous inoculum failed to establish itself which is partly explained by rigorous phytosanitation and partly by unfavourable microclimatic conditions for disease development. Since *P. megakarya* had difficulty establishing itself in the plots, proximity to already infected cacao plantations drove infection dynamics. Thus, isolation of newly established cacao plantations from infected ones and rigorous phytosanitation as a preventive strategy appears to be an effective approach to control black pod for newly established cacao plantations.

Keywords: *Phytophthora megakarya*, primary infections, spatial pattern, temporal evolution, *Theobroma cacao*

Introduction

Cacao (*Theobroma cacao* L.) is an important cash crop in West and Central Africa, the region which accounts for approximately 70% of global cacao production (ICCO, 2014). Production is mainly by smallholder farmers who are facing numerous production constraints, including those due to pests and diseases. Cacao yield losses due to pests and diseases are estimated at around 30% of potential global production (Flood, 2004; Ploetz, 2016). Cacao production in Africa is particularly threatened by two major diseases: cacao black pod rot disease (BPD), caused by two *Phytophthora* species, *P. palmivora* and *P. megakarya* (Akrofi, 2015; Ali *et al*., 2016) and cacao swollen shoot virus (CSSV) disease (Akrofi, 2015; Ploetz 2016). Whereas BPD is of concern in all West African cacao producing countries, CSSV is of particular concern in Côte d'Ivoire, Ghana, Togo and Nigeria (Muller, 2016; Bailey *et al*., 2016).

Cacao black pod rot disease in Africa was first attributed to *P. palmivora* only. However, it became apparent, based on symptoms, morphology, aggressiveness and losses, that other species were involved (Sansome *et al*., 1975, 1979). This led to the description of *P. megakarya* by Brasier and Griffin in 1979. *Phytophthora megakarya* is actually the more aggressive of the two species and can cause up to 80% loss if no control measures are applied (Ali *et al*., 2016; Ndoumbè-Nkeng, 2002). This species is well established in Cameroon, Gabon, Nigeria, and Sao Tome & Principe (Brasier & Griffin, 1979; Nyasse *et al*., 1999) where it seems to have largely or completely displaced *P. palmivora* (Akrofi, 2015; Bailey et al., 2016; Mfegue, 2012). From the border area between Nigeria and Cameroon, *P. megakarya* spread to Togo in 1982, Ghana in 1985, and Côte d'Ivoire in 2003 (Dakwa, 1987; Djiekpor *et al*., 1982; Risterucci *et al*., 2003), where it is still in an invasive phase, coexisting with *P. palmivora*.

Since the identification of *P. megakarya* as a cacao threat, numerous studies have looked at control strategies. Considerable efforts have been made towards cacao resistance breeding and selection, yet no complete resistance to *P. megakarya* has been obtained (Nyassé et al., 2007). Phytosanitation of cacao farms helps to reduce the disease but must be supplemented with other methods (Ndoumbè-Nkeng *et al*., 2004; Nembot *et al*., 2018). Chemical control is the most common method used by farmers to reduce BPD (Deberdt *et al*., 2008; Opoku *et al.,* 2007). Yet due to the many undesirable effects of chemical control on the environment, the health risks for producers and consumers, and the risk for the development of pathogen resistance, more sustainable ways to manage BPD are urgently needed. Integrated pest management (IPM) is increasingly recognised as a workable solution to this problem.

Integrated pest management (IPM) is defined by the EU Framework Directive 2009/128/EC as the careful consideration of all available plant protection methods and subsequent integration of appropriate measures, and emphasises the growth of a healthy crop with the least possible disruption to agro-ecosystems and encourages natural pest control mechanisms (EU directive 2009/2018/EC). Barzman *et al*. (2015) define a set of eight principles to implement in any IPM strategy, where the first of these eight principles is prevention. Disease prevention can be considered as those measures taken to avoid the occurrence of disease but also those to reduce or stop disease progression when established.

The soil is considered the main inoculum reservoir of *P. megakarya*. Inoculum can survive there up to 18 months (Brasier *et al*., 1981; Ward and Griffin, 1981). Primary infections appear at the beginning of the rainy season when inoculum from the soil reaches pods on the tree through splash dispersal (Brasier and Griffin, 1979). Disease symptoms resulting from infection processes are observed on pods in the form of black lesions throughout (Guest, 2007; Nyasse *et al*., 1999). The first symptoms are observed between 2 to 3 days after infection (Akrofi, 2015), followed by a sporulation phase where lesions are covered with mycelium carrying sporangia, mostly within a week after infection (Deberdt *et al*., 2008; Ndoumbè-Nkeng, 2009; Ward and Griffin, 1981). Inoculum derived from sporulating pods can induce secondary infections or inoculum can be returned to the soil. Besides soil, flower cushions, mummified pods, bark, shade trees, and others crops common in cacao plantations have been pointed out as possible inoculum sources of *P. megakarya* (Akrofi, 2015; Akrofi *et al*., 2015; Holmes *et al*., 2003; Opoku *et al*., 2002). It is important to note however, that these have not unequivocally been proven to be alternative sources of primary inoculum.

Temperature, rainfall and humidity are prime determinants for the establishment and dispersal of many pathogens, including *Phytophthora.* Differences in disease occurrence and severity of BPD are partly due to differences in (micro-) climate (Gregory and Madison, 1981; Deberdt *et al*., 2008; Ndoumbè-Nkeng *et al*., 2009). *Phytophthora megakarya* has a short distance dispersal mechanism, mainly through rain-splashing (Gregory, 1974; Gregory *et al*., 1984; Ndoumbe-Nkeng *et al*., 2017; Ristaino. and Gumpertz, 2000; Ten Hoopen *et al*., 2010). *Phytophthora* spp. also need free water for propagule germination and infection and the influence of rainfall on temporal dynamics of BPD has been well documented (e.g. Deberdt *et al*., 2008; Ndoumbè-Nkeng *et al.,* 2009). Yet little is known about how microclimatic conditions, such as temperature and relative humidity, influence spatial disease distribution. Long distance dispersion is also poorly documented. Insects, like ants and beetles as well as rodents and even birds can disseminate *Phytophthora* propagules (e.g. Evans, 1973; Gregory and Maddison, 1981; Gregory *et al*., 1984; Konam and Guest, 2004; Malewski *et al*., 2019). Humans through e.g. contaminated soil on shoes or pruning equipment, may also spread the pathogen (Tjosvold *et al*., 2002). Unfortunately, many of these potential dispersal mechanisms have not (yet) been extensively studied and their relative importance in within-tree (vertical and especially upwards) and between trees (horizontal) dispersal of *P. megakarya* needs to be further elucidated.

Knowledge on dispersal mechanisms is essential to improve control of *P. megakarya* by providing the possibilities of preventing arrival and spread of disease. However, dispersal is difficult to measure in natural agro-systems (Bullock *et al*., 2006). Knowledge of spatial patterns allows to generate hypotheses on the underlying dispersal mechanisms that occur in the field (Dale, 1999). Moreover, spatial pattern analysis could provide quantitative information on population dynamics of pathogens and help with experimental design and sampling programs in epidemiological research (Campbell & Madden, 1990). Epidemics caused by *Phytophthora* species are often initially patchy in appearance.

This reflects the impact of environmental and genetic heterogeneity and *Phytophthora* population growth upon the processes of reproduction, dispersal, and mortality (Ristaino and Gumpertz, 2000).

Few studies looked at spatiotemporal dynamics of BPD. Moreover, the few existing studies (Ndoumbe-Nkeng *et al.,* 2017; Ten Hoopen *et al*., 2010) were carried out in cacao farms where *P. megakarya* was already well established. Since observed spatial patterns are often related to past processes that give rise to them, it is difficult in such plantations to hypothesise on some of the underlying processes, especially regarding primary infections and disease establishment. Studying spatial and temporal dynamics of BPD in farms initially devoid of endogenous inoculum can provide relevant information that could help to avoid arrival of *P. megakarya* inoculum and to halt disease spread once established.

Therefore, the objective of this study was to gain information on dispersal mechanisms of *P. megakarya* as well as factors involved in disease establishment in newly planted cacao plots by describing: i) the spatial pattern of primary infections, ii) the spatial autocorrelation of such infections, and iii) their progression over time.

Materials and Methods

Description of experimental site

The study was carried out over the period 2009 to 2016 on three smallholder plots located in the Centre region of Cameroon. Plots were located in three villages: Bakoa, Kédia, and Ngat. All villages are in the bimodal rainforest agro-ecological zone, characterised by a relatively intense dry season from November to March, followed by a short wet season from March/April to May/June, a short dry season from June to August and a long wet season from August to November. The main cacao production cycle generally starts with flowering after the first rains in March/April (short wet season) and ends in November/December of the same year sometimes overflowing into January. Bakoa and Kédia are localised in the forest-savannah transitional zone at 4°34’N, 11°09’E, 450 masl and 4°29’N, 11°29’E, 470 masl, respectively with mean temperatures ranging from 20 to 30 °C and rainfall of about 1100 mm per year. Vegetation is made up of gallery forest and grassland (Jagoret *et al*., 2012). Ngat is located in a typical forest zone at 3°46’N, 11°49’E, 700 masl and is more humid than the forest-savannah transitional zone. Mean temperature range from 20 to 25 °C and rainfall is about 1600 mm per year. The initial vegetation is forest, which is currently progressively being replaced by a more agricultural landscape.

The smallholder plots were installed in 2006 using cacao germplasm consisting of newly developed hybrids and farmer selected planting materials, which are to be assessed for their productivity and possibly disease resistance under farmer field conditions. Full-sib seedlings obtained through a single crossbreeding between parents with known resistance levels to *P. megakarya* or grafted clonal materials (mostly farmer selections or cacao varieties with known resistance to *P. megakarya* used as control, such as SNK10) were planted mainly in lines and separated from others by perennial companion

crops. For a list of the hybrids and farmer selected planting materials see e-Xtra 1. Cacao plots were installed on unshaded land (deforested areas or savannah) that had not harboured cacao trees for at least 20 years. Cacao and companion trees were planted at the same time. For the first two to three years after planting, shade was provided by *Musa* spp. (banana and plantain) since the companion tree crops at the time of planting (2006) were of similar size as the cacao trees.

In Bakoa, two contiguous plots were selected, 57 x 72 m and 45 x 54 m (Fig. 1a), where a total of 594 cacao trees were intercropped with either coconut (*Cocos nucifera*) or African oil palm trees (*Elaeis guineensis*). These companion trees were planted at 12 x 7.5 m with three continuous lines of cacao trees spaced 3 x 3 m in between. These plots were surrounded by an old (>20 years), well managed agroforestry based cacao plantation where *P. megakarya* was already well established (Fig. 1A). Although the two Bakoa plots differed slightly in layout and were intercropped with different species, since they were contiguous, they were considered as one single plot with a total area of 117 x 57 m.

Two plots of 66 x 76 m and 48 x 69 m were selected respectively in Kédia and Ngat. A total of 354 cacao trees were intercropped with African oil palm planted at 14 x 7.5 m in Kédia (Fig. 1B) while fruit trees (*Citrus* spp*, Persea americana* and *Dacryodes edulis*) were used in Ngat and planted at 6 x 12 m with 352 cacao trees (Fig. 1C). The Kédia plot was surrounded at its southern site by a river, at its eastern side by an old cacao plantation (>15 years) and the other sides by newly established cacao farms (>5 years) (Fig. 1B). The Ngat plot was surrounded on three sides by densely overgrown abandoned cacao (>30 years) and on one side by annual crops which were later replaced by a similar cacao plot as the one studied. Fruit trees replaced a cacao tree whereas oil palm and coconut trees were planted on separate lines (Fig. 1C). The Kédia and Ngat plots were established on a slight slope (Figs. 1B and 1C). In all three locations, *P. megakarya* was present in the surrounding environment/cacao plantations at the moment of installation and throughout the observational period (2009-2016).

It is important to note that this study was carried out on farmer fields. These cacao plantations represent a considerable farmers' investment and contribute significantly to the livelihood of these farmers. Consequently, farm management decisions were primarily in the hands of the farmer, contrary to on-station trials. Even though farmers were willing to avoid as much as possible fungicide sprays in order to accommodate the research, in two cases they decided to apply fungicides. In Bakoa, a copper based fungicide (Kocide, a.i. copper-hydroxide), was applied preventively at least twice during the 2013 production season. In Kédia, a single preventive treatment (a.i. copper hydroxide) took place after a flooding event in 2014.

Data collection

From June 2009 to December 2016, all cacao plots were closely monitored in order to detect *P. megakarya* infections. Assessment of disease severity by counting total number of healthy and infected pods per tree would have been very time consuming since each plot has >300 cacao trees. Thus observations focused on the presence or absence of cacao pods and disease incidence, i.e. the presence

(1) or absence (0) of infected pods on a tree. These observations were done by local observers once a week for each cacao tree. Unfortunately, due to logistical problems the data sets for 2012 for all three plots were incomplete and this year was excluded from the analyses.

When a *P. megakarya* infection was present, rotten pod(s) was/were removed from the tree. This was done to eliminate as much as possible secondary inoculum which would allow a better understanding of the relative importance of primary inoculum on disease occurrence and spread. On a weekly or monthly basis, the total number of productive and/or diseased trees were generally too low to allow for meaningful temporal or spatial analyses. The data were therefore pooled on a yearly basis for analyses. At the end of each main production cycle (which coincides in general with calendar year) a status for each cacao tree was defined as follows (considering the whole production cycle) 1) "Non-Productive" for trees with no cacao pods (or dead trees), 2) "Healthy" for trees harbouring only non-infected pods and 3) "Infected" for trees harbouring at least one infected pod. This allowed us to visualize the distribution of *P. megakarya* infections in each plot per calendar year using the plantation layout maps (Fig. 1).

It is important to mention that in Cameroon, the only plant organs visibly affected by *P. megakarya* are the cacao pods, contrary to *P. palmivora* that causes not only pod rot but also cankers and leaf blight in cacao. Thus cacao trees change health status within and between years based on the presence or absence of healthy and rotten pods.

In June 2009, before the appearance of any rotten pods, 20 soil samples, spread out evenly throughout the plots, were collected in Bakoa, 10 in Kédia and 10 in Ngat, to test for the presence of *P. megakarya*, according to the method described by Mfegue (2012) and Ndoungué *et al*. (2018). Subsequent soil sampling, from 2010 till the end of 2016, was done twice a year, once during the large dry season and once during the large wet season. Soil samples were taken throughout the whole plantation at the foot of trees that were classed either as "Healthy" or "Infected" the previous year. The number of samples varied per plot and between years, depending largely on the number of "Infected" trees in the year previous to the sampling year. Soil sample locations are given in Fig. 1. Three hypotheses were tested:

- H1 Pathogen presence in the soil in year $t+1$ is related to disease incidence in year t
- H2 disease incidence in year $t+1$ is related to disease incidence in year t
- H3 Pathogen presence in the soil in year $t+1$ is related to presence in the soil in year t

The relationships between soil samples testing negative (0) or positive (1) for the presence of *P. megakarya* and cacao tree status, healthy (0) or infected (1) were analysed by calculating the odds ratio using two dimensional contingency tables. Because of low numbers expected in some cells of the contingency table, the one-sided Fisher Exact test (Agresti, 2007) was used.

Spatial disease pattern and correlation

Spatial disease patterns were analysed using Ripley's K(r) function which is increasingly being used in ecological and epidemiological studies (Gidoin *et al*., 2014; Jolles *et al*., 2002; Ngo Bieng *et al*., 2013; Oro *et al*., 2012; Solla and Camarero, 2006). Ripley's function was shown to be appropriate for analysing point processes (Cressie, 1993) and was used to determine spatial distribution of "Infected" cacao trees at plot scale.

Ripley's K(r) is a tool for analysing a completely mapped spatial point process, e.g. data on the location of events. K(r) describes the characteristics of the point processes over a range of scales. The function is $K(r) = \lambda^{-1}E$, where E (r) = expected mean number of points within a distance *r* of a randomly chosen point and λ is the density (number of points i.e. infected trees per unit of area) on the studied plot. Since distance between "Infected" cacao trees and the number of points per unit area (λ) are used in the analysis, possible effects of the spatial layout of the plots are integrated in the results.

For the Poisson process, which serves as a null hypothesis $K(r) = \pi r^2$, the spatial pattern is random. For an aggregated pattern, it is expected that points have on average more neighbours than for the null hypothesis, and thus $K(r) > \pi r^2$. Conversely, for a regular process the points would have on average fewer neighbours than for the null hypothesis, then $K(r) < \pi r^2$.

To facilitate interpretation, Besag (1977) defined a linearized modified K(r) function as $L(r) = \sqrt{\frac{K(r)}{\pi}} - r$, where L(r) = 0 at all distances *r* for random processes, L(r)> 0 for aggregated processes and L(r) <0 for regular processes.

However, the above K and L functions underestimate the values of K(r) and L(r) because of the points located near the borders, which have fewer neighbours than other points in the study area (Goreaud, 2000). To avoid misinterpretation due to the border effect, it is advisable to use r-values corresponding to a quarter or half of the width of the study area (Goreaud, 2000). In this study, as the edge lengths of the plots were all comprised between 40 and 80 m, an r-value of 20 m was used.

Here we were interested in the spatial structure of "Infected" cacao trees, and since cacao trees in this study were regularly distributed, they were considered as the reference population. The significance of the determined pattern was assessed through a comparison to a classic null hypothesis of complete spatial random distribution, following the Monte Carlo Method (Besag & Diggle 1977 in Goreaud, 2000; Landcaster & Downes, 2004). A confidence interval of L(r) at the 0.01 level for each of the three plots through 10 000 random permutations of healthy and infected trees was build. The analyses were performed by year when at least ten infected trees were present within a plot.

Join count statistics was used to characterise the relative location of infected cacao trees similarly to Bonnot *et al.* (2010) and Oro *et al*. (2012) in order to provide information on the directionality of infections. These statistics measure association by counting the number of pairs of trees separated by a given distance and orientation that are both diseased (D-D), the number of pairs of trees that are healthy (H-H), and the number of pairs in which one tree is diseased and one is not (D-H). These

counts can be performed following many spatial proximity patterns: within rows (vertically), across rows (horizontally), diagonally or a combination of these at different distances (Cliff and Ord, 1981; Reynolds and Madden, 1988). The observed number of joins is compared to the expected one under the null hypothesis of no spatial autocorrelation to determine whether the association is statistically significant.

For each plot and each year with *d* infected cacao trees (D), the D-D join count statistic was calculated for each pair of infected cacao trees separated by a distance *x* across rows and *y* along the row. The null distribution under the hypothesis of no spatial autocorrelation was obtained by randomly assigning *d* diseased trees in the plot and calculating the D-D join count for each (*x, y*) class. This was done through 1000 permutations of observed data. For each field and year, a p-value was obtained for each (*x, y*) class by comparing the D-D statistic of the observed data to the corresponding null distribution. The set of all obtained p-values was used to build a 2D correlogram with $-30 \leq x \leq 30$ and $y \leq 30$ (negative values of *y* need not be plotted since the complete correlogram is symmetrical with respect to the origin because (*x, y*) and (*y, x*) correspond to the same class). The analysis does not assume that the rows are regularly spaced: irregularly spaced rows (e.g. in Kédia plot) produce irregularly spaced correlograms that represent correctly the distance classes.

Special attention was given to differences in vertical versus horizontal spatial autocorrelation for the Bakoa and Kédia plots, where cacao is intercropped with coconut or oil palm, this in order to see whether these crops and their spacing could provide a barrier to *P. megakarya* dispersal.

Temporal disease dynamics

Since weekly disease incidence was low, temporal disease dynamics was considered at a yearly basis yet differentiation between infections due to primary or secondary inoculum was done using weekly data. Primary infections were defined as infections caused by primary inoculum from an environmental reservoir, such as the soil or e.g. the surrounding environment of the cacao plots. Secondary infections were defined as those infections that stem from infected pods within the cacao plot, producing secondary inoculum. At the individual tree level three hypotheses were tested:

- H4 - secondary infections in year *t* derive from primary infections in year *t*;
- H5 - the number of primary infections in year *t+1* is determined by the number of infected trees in year *t* ;
- H6 - primary infections in year *t+1* are generated by secondary infections in year *t*.

Temporal disease dynamics was studied by looking at the relative importance of infections due to primary and secondary inoculum over years. Several assumptions were made to differentiate infections due to primary or secondary inoculum with reference to previous studies (Gregory and Maddison, 1981; Ndoumbè Nkeng *et al.,* 2002; 2017; Ten Hoopen *et al*., 2010). Primary inoculum is responsible for the first infection in each year. Given the limited distance over which rain-splash dispersal occurs (Gregory *et al*., 1984; Gregory and Maddison, 1981; Ten Hoopen *et al*., 2010), at plot level all infections occurring

292 at distances of 6 m or more were also considered to be due to primary inoculum. At the level of the
293 cacao tree, recurrent infections separated by more than two weeks were considered to be independent of
294 the previous infection, given that the latent period is approximately 1 week (Akrofi, 2015; Bailey *et al*.,
295 2016). Any infection occurring within two weeks and at distances less than 6 m from previous infections,
296 were considered to be due to secondary inoculum. Based on these assumptions, the number of primary
297 and secondary infections was estimated for each year. The analysis was performed for individual plots
298 as well as on data from all plots together using two dimensional contingency tables. The one-sided Fisher
299 Exact test (Agresti, 2007) was used since it is adapted to rare events.
300 All analyses were carried out in R, version 3.3.1 software (R Core Team, 2013). The Ripley
301 function was obtained using the ads package (Pélissier and Goreaud, 2010), the join count analysis was
302 performed by programming, data from the soil samples and the temporal dynamics of primary and
303 secondary inoculum was tested using the exact 2 x 2 package (Fay *et al*., 2018).
304
305 ***Temperature and relative humidity***
306 In order to see whether observed spatial patterns could be (partially) explained by intra-plot
307 microclimatic variability, a total of 28 Tinytag plus 2 data loggers (TGP450, Gemini Data loggers, UK)
308 were used to register temperature and relative humidity at different locations in each plot (13, 6, and 9
309 data loggers in Bakoa, Kédia and Ngat, respectively). Calibration of data loggers was checked prior to
310 their utilisation by comparing readings to a Vantage Pro 2 (Davis, CA, US) weather station. Although
311 rainfall is a primary factor in *P. megakarya* dispersal and explains for a large part temporal patterns at
312 plot scale (e.g. Deberdt *et al*., 2008, Ndoumbé-Nkeng *et al*., 2009), here, it was considered less important
313 with regard to spatial patterns at plot scale. Moreover, rainfall measurements at microclimate scale
314 (intra-plot differences in rainfall) were outside the scope of the project and rainfall was thus not recorded.
315 The locations of the data-loggers were coded as follows: B1 to B13 for the Bakoa plot, K1 to
316 K6 for the Kédia plot and N1 to N9 for the Ngat plot. Data-loggers were placed regularly throughout
317 the plots in order to capture overall microclimatic variability (Fig. 1). Each data logger was placed in
318 the canopy of a cacao tree approximately 2 m above ground level, which corresponded to the lower
319 branches of the cacao tree canopy (cacao trees were approximately 4-5 m high). Data were registered
320 every 30 minutes from 15 June to 30 November 2016, which corresponds to the large rainy season and
321 generally the period where BPD is most prevalent. Data loggers B3 (Bakoa), N2 and N3 (Ngat)
322 malfunctioned and their data were discarded.
323 The microclimatic variables chosen for analysis for the period under observation were mean
324 maximum daily temperature T_{max}, given that *P. megakarya* has a relatively low optimum growth
325 temperature for a tropical pathogen compared with for example *P. palmivora* (Puig *et al*. 2018); the
326 mean time in hours per day ($h.d^{-1}$) that temperature was above 30 °C, the temperature at which *P.*
327 *megakarya* stops growth (Puig *et al*. 2018); mean daily minimum relative humidity (RH_{min}); and the

mean daily relative humidity amplitude (difference between daily max and min relative humidity) given that humidity is an important factor in BPD epidemics (Monteith and Butler 1979; Butler, 1980).

The Kruskal-Wallis test and the Wilcoxon rank test were used to compare the distribution of T_{max}, RH_{min} and their amplitudes, T_{ampl} and $RH_{ampl,}$ recorded at each point within the registered period. The same analysis was used to compare plots. This was done to see whether the micro-climatic conditions were similar within or between plots and if not, whether these differences could help explain observed spatial patterns of disease occurrence.

Results

Phytophthora megakarya arrival and soil samples

All 2009 soil samples tested negative for the presence of *P. megakarya*. Plot layout maps illustrating spatial distributions of infections and the results from the soil sampling for each plot for each year are shown in Fig. 1. The arrival of BPD infections occurred at different times in the plots. First infections were observed at the end of 2009 in Ngat on two cacao trees (Fig. 1C), followed in 2010 by the plot in Bakoa where infections appeared on 12 trees (Fig. 1A). BPD was noted in 2011 in Kédia on 13 trees (Fig. 1B). After the appearance of first infections in each plot, subsequent disease spread differed when looking at the evolution of spatial distributions of infected trees over time.

The number and percentage of soil samples that tested positive for the presence of *P. megakarya* per plot and per year varied between plots and years. In Bakoa the first positive soil samples were found the same year the disease was first observed on cacao pods (Fig. 1A). In Kédia and Ngat the first positive soil samples were collected the year following the arrival of the disease (Fig. 1B, C).

Since the one-sided Fisher test used to determine associations between soil infestation and disease incidence showed similar results for individual plots (data not shown) compared with pooled data from all plots, only the results for pooled data are presented (Table 1). The analyses show that only in two cases 2013-14 and 2014-15, disease incidence was significantly linked to soil infestation the following year (Table 1, H1). Moreover, it showed that disease incidence in year *t* was significantly linked to disease incidence the following year (*t+1*) (Table 1, H2) and that soil infestation was only significantly linked to soil infestation the following year for the final years of observation, 2015-2016 (Table 1, H3).

Spatial disease pattern and correlation

For the Bakoa plot (Fig. 2a), in 2010, L(r) values did not exceed the confidence interval, therefore we could not reject the null hypothesis of complete spatial randomness of infected trees. From 2011 to 2016, Bakoa showed significant positive L(r) values for $r > 5$ m (Fig. 2A), spatial disease patterns were thus aggregated these 5 years. When looking at the distribution of infected trees over time (Fig. 1A), it becomes apparent that the locations of the clusters of infected trees varied between years. In other words, there were no clusters of infected trees that were consistently located at similar positions over time.

In Kédia, from the appearance of infections in 2011 until 2016, all L(r) function curves displayed significant positive values meaning that the observed disease patterns were aggregated (Fig. 2B). In 2011 and 2013 most infections were localised in the Eastern part of the plot, close to the river (Fig. 1B). In 2014, the flooding event caused a more even distribution of infections throughout the lower part of the plot (the part actually inundated, closest to the river). It is interesting to mention that up till the flooding event most infections (n=13) were localised in the Eastern part of the plot, as in 2011 and 2013 (data not shown). Moreover, it is important to mention that the river flows from East to South. In 2015 and 2016, infected trees were localised in the South east of the plot, slightly more towards the south when compared with previous years (Fig. 1B).

In Ngat, for those years that the analysis was possible (more than 10 infected trees) the disease pattern was always aggregated (Fig. 2C). Apart from 2009, all infections were located towards the Eastern part of plot whereas in 2016 an additional cluster was observed in the southern part (Fig. 1C).

Generally, aggregated patterns of infected trees were observed (Fig. 2). Although the distribution of infected tree clusters varied slightly between years, especially in Bakoa, there was a consistency in location of certain clusters of infected trees. This consistency was most pronounced in Kédia and Ngat.

For the results of the join count statistic, only those positive spatial autocorrelations (PSA) attached to the core cluster, in the centre of the correlogram, were of interest. PSA not attached to the core cluster are rare events, unlikely to occur. Significant positive PSA were found in all plots for most years. No negative PSA were found. Core cluster size ranged from 3-18 meters, yet was on average 3-9 m (Fig. 3). Cluster size generally increased over time (Fig. 3). In Bakoa the direction of the PSA was on the x-axis in 2010 and slightly more on the y-axis from 2011 to 2016, meaning that a PSA was more evident within rows than across rows (Fig. 3a).

PSA were also detected for all years in Kédia with a slightly more vertical aspect (along the y-axis) than horizontal (along the x-axis) except for 2015 and 2016 (Fig. 3B). Since in Kédia the slope of the plot is upwards away from the river (Fig. 1B), this vertical aspect can not be explained by dispersal through run-off water which was directed towards the river (river and run-off water tested positive for the presence of *P. megakarya*, data not shown). For Ngat, no correlation was found in 2009. From 2010 to 2016, significant PSA were detected. A more vertical (along the y-axis) distribution of PSA was found in 2010 and from 2013-2015, a more horizontal (along the x-axis) distribution was observed in 2011 and 2016 (Fig. 3C). Contrary to Kédia, in Ngat this more vertical distribution is likely linked to run-off water along the slope of the plot from south to north (Fig. 1C).

Temporal disease evolution

When looking at the evolution of the number of infected trees over time, in Bakoa and Kédia numbers fluctuated whereas in Ngat it generally increased (Fig. 4). In Bakoa, after the first 12 diseased trees observed in 2010, the number of diseased trees varied from 19 in 2011 to 89 (highest) in 2013. In Kédia,

the number of infected trees fluctuated around 25 from 2011 to 2016, except in 2014 when it reached 137. Actually, in 2014 until 4 November, 13 infected trees were observed, then, after heavy rainfall led to flooding up to 36 m from the river into the plot, the number of infected trees increased to 67 and finally to 137 at the end of 2014. In Ngat, two diseased trees were observed in 2009 and 2010. This number gradually increased to 15 in 2011 and finally 38 in 2016 (Fig. 4).

Temporal representation of primary and secondary infections (Fig. 5) show that BPD was most predominant during the large wet season of each year (September to November). Primary inoculum initiates not only epidemics but continues to induce infections throughout the year (Fig 5). However, in most instances towards the end of the production season, secondary infections become more prevalent. This is especially clear in Bakoa for the years 2011-2016 (Fig 5A), for the Kédia plot in years 2013 and 2016 (Fig. 5B) and Ngat (Fig. 5C) in 2011, 2014 and 2016. Interestingly, in Kédia and Ngat in 2015 (Figs 5B and C, respectively) basically all infections were considered primary infections.

Since the one-sided Fisher test used to determine associations between primary and secondary infections at the individual tree level, showed similar results for individual plots (data not shown) compared with pooled data from all plots, only the results for pooled data are presented (Table 2). The analyses show that at the level of the individual tree, most secondary infections were derived from primary ones and few from non-primary infections (Table 2, H4). Moreover, it showed that primary infections in year *t+1* were significantly linked to the infected trees of the previous year *(t)* (Table 2, H5) and mainly to those with secondary infections (Table 2, H6) in that year (*t)*.

Temperature and relative humidity

When looking at the microclimatic variables, significant difference (*P<0.0001*) was observed between plots (Table 3). Mean daily time (in hours day^{-1}) that temperature was > 30 °C, shows that Kédia was the hottest locality (with 5.5 hour.day^{-1}), followed by Bakoa (4.5 hour.day^{-1}) and Ngat the coolest one with absence of temperatures exceeding 30°C during the period of data collection.

For all microclimate variables, significant differences between microclimate measuring points were observed in all plots (Table 3). In Bakoa $T_{>30}$, T_{max} and T_{ampl} were lower in B6, B7 and B9 compared with the other points while in point B7 a high RH_{max} with small RH_{ampl} was registered (84.1 % with 14.9 %). Interestingly, locations B7 and B9 showed recurrent infections. However, a high number of infected trees was observed in 2013 at location B6. In Kédia, the coolest location was K4 located in the main infection area. The average values obtained were respectively 3.5 hour.day^{-1}, 31.8°C and 11.6°C for $T_{>30}$, T_{max} and T_{ampl}, and 63.0% and 37.6% for RH_{min} and RH_{ampl}. In Ngat, when compared with the other plots, relatively low $T_{>30}$, and $T_{max.}$ were observed. The coolest point of the plot was N1 with no temperature above 30°C ($T_{>30}$ = 0), T_{max} and T_{ampl} were 26.5°C and 6.9°C and RH_{min} and RH_{ampl}, were 68.7% and 29.9%, respectively. Although location N1displayed the most optimal microclimatic conditions for BPD, it was located at the opposite site of the main disease area.

438 **Discussion**

439 The aim of this study was to describe spatial and temporal dynamics of *P. megakarya* infections in newly
440 established cacao plantations and to test six hypotheses on the processes involved in *P. megakarya*
441 dispersal and establishment. Since all soil samples collected in all plots before the arrival of first
442 infections tested negative for the presence of *P. megakarya*, inoculum responsible for the first infections
443 (2009 Ngat, 2010 Bakoa, 2011 Kédia) was of exogenous origin. In the surrounding environment of all
444 three plots, "old" cacao affected by *P. megakarya* was present and thus very likely at the origin of these
445 first infections.

446 Looking at the spatial patterns and correlations of infected trees in the three plots for the years when
447 first infections were observed, random, aggregated or undetermined pattern of infections and few or no
448 PSA were found. Over time, all infection patterns became aggregated and more PSA were detected, with
449 mean core clusters of 3-9 meters. PSA are governed by 1) dispersal and/or 2) the environment (Koenig,
450 1999). Given the short natural dispersal distance mechanism due to rain-splashing of *P. megakarya*
451 (Gregory & Madison, 1981), and the weekly removal of infected pods, which limits secondary infections
452 (Nembot *et al*., 2018) this explains the small core cluster size. These results do indicate however, given
453 the aggregated patterns and PSA, that disease spread is step by step to neighbours of infected trees. This
454 spatial pattern of BPD has also been observed in relatively old infected cacao plantations (Mfegue, 2012;
455 Ndoumbè-Nkeng *et al*., 2017; Ten Hoopen *et al*., 2010).

456 The intra-plot environment, especially the presence of coconut and oil palm trees in Bakoa and
457 Kédia and the presence of a slope in Kédia and Ngat seemed to influence the direction of PSA. Given
458 that the palm trees were planted on separate lines, this increases the distance over which dispersal of
459 secondary inoculum should take place between cacao trees on opposite sides of the palm trees, thereby
460 presenting a barrier to horizontal intra-plot dispersal. The presence of a slope facilitates dispersal
461 through run-off water. In the case of Ngat this led to an increase in infections along the slope, whereas
462 in the case of Kédia, it did not, since the slope went upwards from the area with most infections.

463 It was expected that over time, an increase in infected trees would lead to larger areas of
464 contiguous infected trees leading to PSA clusters of larger size. This however, was not the case for
465 Bakoa, whereas this seemed to occur, albeit on a limited scale, in Kédia and Ngat. The question therefore
466 is, why did the number of infected trees remain relatively low and did not continuously increase over
467 time as expected? Although variability in annual rainfall distribution and quantity could explain
468 differences in number of infected trees between years, as the flooding event in 2014 clearly
469 demonstrates, it does not explain why the number of infected trees remained relatively low in all three
470 plots. Two potential explanations come to mind, weekly phytosanitation and fungicide treatments, the
471 latter being a factor to take into careful consideration when interpreting the results. In Bakoa (in 2013)
472 and Kédia (in 2014), fungicides were sprayed on a preventive basis. In both cases, the subsequent year
473 showed a decrease in total number of infected trees. In the case of Kédia this decrease was quite
474 substantial. Yet, in well-established infected cacao plantations, phytosanitation and fungicide spraying

do not normally cause such a drastic reduction in black pod rot as observed here. Weekly phytosanitation is insufficient to eliminate secondary inoculum production completely (Ndoumbé Nkeng *et al.* 2004; Nembot *et al*., 2018; Opoku et al. 2007). Ndoumbé Nkeng *et al.* (2004) even found higher pod rot levels after rigorous phytosanitation efforts the year before. Moreover, the fungicide used here, a copper based contact fungicide, was applied only once in Kédia and twice in Bakoa. The fungicide leaches off in two to three weeks, after which it does not continue to exert control.

It thus seems that in this case, when the disease is not yet well established, phytosanitation (and possibly fungicide treatments) might be more effective compared with conditions where the disease is already well established. The reason for this lies within the soil. Rotten pods produce secondary inoculum that through a leaching process reaches the ground and, through a poorly understood process, is incorporated into a soil inoculum reservoir, which is the principal source of infections besides sporulating pods (Gregory et al., 1984). From there it can re-infect cacao pods. Phytosanitation and fungicide sprays reduce the amount of secondary inoculum produced and thus its incorporation into a soil inoculum reservoir. Whereas in older plantations soil inoculum is ubiquitous and thus provides a continuous endogenous source of inoculum even when phytosanitation occurs, in newly planted plantations as here, this inoculum reservoir has to build up.

This idea is further supported by the finding that only in one case (2015-2016) a significantly link for soil infestations between years was found. This idea is also supported by data from Ndoungué *et al*. (2018) which showed that in a plantation >20 years old, where *P. megakarya* was already well established, out of 18 soil samples, 16 (>88%) tested positive for *P. megakarya*. Since in the Ndoungué *et al.* (2018) study for each sample (n=18) three subsamples were taken to check for the presence of *P. megakarya,* it could be argued that this would lead to an overestimation compared with this study. However, when looking at the number of subsamples (3 x 18, n=54), 32 (> 59%) of these tested positive for *P. megakarya*. In this study, out of 1479 soil samples, only 173 (11.7%) tested positive for *P. megakarya*. Even when only looking at soil samples taken at the foot of trees that actually had BPD the year before, out of 556 samples, only 120 (21.6%) tested positive for *P. megakarya* (see *e*-Xtra 2).

When disease incidence is low, farmers normally do not rigorously control BPD by phytosanitation or fungicide spraying. It thus seems that the rigorous phytosanitation employed in this study, prevented the build-up of a soil inoculum reservoir explaining the slow disease progression.

In Ngat, despite the relatively more favourable microclimatic conditions for BPD spread and the absence of fungicide applications, there was also a relatively low number of diseased trees. Besides phytosanitation, this could also be explained by the very low productivity of this plot, with a relatively high number of unproductive trees. Whereas productivity was >1 kg of dry cocoa beans per cacao tree in Bakoa and Kédia, it was less than 0.2 kg in Ngat (based on data from 2013-2017; O. Sounigo, pers, comm). The low productivity and relatively high number of non-productive trees in Ngat is due to the impact of a cacao mirid (*Sahlbergella singularis*) on production capacity of cacao trees. A study on mirid distribution and their damages in 2009 and 2010 in six cacao plots showed that density and damage

was high in the Ngat plot compared to other studied plots (Mahob *et al.*, 2015). Beilhe *et al*., (2017) showed that losses due to mirid attacks are not limited to pod damage but impact negatively on the productive capacity of trees. Fewer pods means fewer host organs for *P. megakarya* to infect.

Rainfall is a prime explanatory variable for temporal patterns of infections and is linked to the number of infected trees within a plot (Deberdt *et al*., 2008, Ndoumbé-Nkeng *et al*., 2009, 2017). However, overall rainfall data does not explain spatial variability within plots. The microclimatic environment influences establishment and spatial distribution of the disease in the plots. Although the available data presented here prevents us from establishing definitive causal relationships with disease distribution, indications of the impact of micro-climate on disease distribution were found. Naturally, the savannah environment (in Bakoa and Kédia) presents a less conducive environment for black pod rot disease development than the forest environment (Ngat). Interestingly, *P. megakarya* being a tropical pathogen, it actually has a relatively low temperature optimum, between 23-26 °C (and no growth above 30 °C) (Brasier and Griffin, 1979; Puig *et al*., 2018), conditions which are clearly more often observed in the forest than the savannah environment. Despite the fact that mean maximum temperature in the savannah plots was over 30°C, corresponding to the threshold at which *P. megakarya* starts losing its viability *in vitro* (Puig *et al*., 2018), the occurrence of disease took place. Although it is unlikely that lethal temperatures are maintained in cacao fields for sufficient duration of time to eliminate *P. megakarya,* temperatures of 30 °C or more, which reduces *P. megakarya* growth, are more common in the unshaded versus shaded conditions and in savannah versus the forest plots, which could explain intra- and inter-plots differences in occurrences. However, it is important to note that temperature is influenced by other meteorological factors such as wind speed, vegetation and topography. Similarly, humidity is influenced by plot structural and topographical features. Medeiros (1967) showed that shaded plantations in humid areas such as river valleys appear to be more prone to disease than well ventilated plantations in neighbouring areas receiving similar rainfall.

When comparing between years, the location of infection clusters was most consistent in Kédia and Ngat, and the location of infection clusters was more variable in Bakoa. When looking at the - data for the Bakoa plot, there did not seem to be a particular area which was consistently infected. This is also reflected in the micro-climate data which did not show any part of the plot having optimal micro-climatic conditions for *P. megakarya* development. In Kédia, microclimate was most conducive for disease development in the eastern part of the plot where infections were consistently observed. This is not surprising given the relative favourable environment provided by the river and the shade provided by the tree border alongside the river bank. Finally, in Ngat microclimate was generally more conducive to *P. megakarya* development, compared with the other two plots, and intra-plot differences were less pronounced. However, infections were mostly located in the eastern part of the plot. This part of plot receives more shade in the morning compared to other parts of the plot. This could induce dew to remain on pods after sunrise for a more extended amount of time, facilitating the germination of spores of *P.*

548 *megakarya*. Monteith & Butler (1979) showed that persistent dew on the pod surface for up to 3 hours
549 after sunrise are ideal conditions for BPD development.
550 Temporal dynamics of primary and secondary infections revealed that secondary infections
551 were most often derived from primary ones than from other infections. Since this result was obtained at
552 the individual tree level, it indicates that there was more within than between trees dispersal. Moreover,
553 most infected trees generated secondary or primary inoculum that contributed to them being infected
554 within the same or the following year. The lack of increase of the total number of infected trees over
555 time is thus because secondary inoculum mainly causes self-infection but fails to disperse between trees.
556 This supports the hypothesis emitted by Ten Hoopen *et al*. (2010) who stated that primary inoculum is
557 the main determinant for the spatial development of an epidemic at the plantation level and that
558 secondary inoculum is mainly responsible for the within-tree temporal development of an epidemic.
559 However, given the weekly removal of diseased pods, care has to be taken comparing this to situations
560 where secondary inoculum is abundant.
561 The results also indicate that primary inoculum does not only initiate the epidemic but continues
562 to induce infections throughout the year(s). The exact Fisher test performed for individual plots (data
563 not shown) and the combined data from all plots confirmed this hypothesis and these results are in line
564 with Nembot *et al*. (2018) who also demonstrate the importance of primary inoculum in *P. megakarya*
565 disease epidemics. Moreover, in all plots and throughout the years, primary infections occur at distances
566 of over 6 meters from any given potential inoculum source. This indicates that long range dispersal plays
567 an important role, at least in the early years, in epidemics.
568 Studying population dynamics of *P. megakarya* can help to detect the introduction of exogenous
569 inoculum and could provide information on the origins of exogenous inoculum. Interestingly, the
570 flooding event that occurred in 2014 in Kédia caused a large increase in number of infected trees, most
571 of these located in the lower part of the plot that was actually flooded (up to 36 m into the plot). Since
572 there were infected pods prior to the flooding event, the question remains whether the flooding caused
573 endogenous inoculum to be dispersed, whether exogenous inoculum was brought in by the river (river
574 water tested positive for the presence of *P. megakarya*, data not shown), or both. Interestingly, water
575 samples from the river before the flooding tested positive for *P. megakarya* (data not shown) and thus
576 the flooding event more than likely introduced exogenous inoculum. It is known that many
577 *Phytophthora* spp such as *P. ramorum*, *P.* x *alni*, and *P. parasitica* are dispersed by streams & rivers
578 (Jung & Blaschke, 2004; Neher & Duniway, 1992; Themann *et al*., 2002) yet to our knowledge this is
579 the first time this is also shown to be true for *P. megakarya*. It is important to note that the flooding
580 event in Kédia in 2014, actually brought into play a second dispersal mechanism, besides rain-splash,
581 and the assumptions made to distinguish between primary and secondary infections where thus not valid
582 anymore as of the date of the flooding event. Eliminating these data from the Fisher exact test did not
583 however, change the outcome of the results, showing that the observed effects are robust.

584 This flooding event demonstrates one of the mechanisms for long range dispersal. Other long
585 range dispersal mechanisms include e.g. ants. Although the role of ants in establishing BPD infections
586 has been determined (Evans, 1973; Gregory *et al*., 1984; Ngwohgi, 2015) the distance over which they
587 might transport inoculum (horizontally and vertically) remains unclear. Finally, the possibility of
588 human, rodent, flying insect or even bird mediated transport of inoculum should not be neglected either
589 (Tjosvold *et al*., 2002; Konam and Guest, 2004; Malewski *et al*., 2019) and merits further attention. The
590 continued presence of a disease cluster as of 2010 in the Ngat plot next to a footpath through the plot
591 might present a clue as to the importance of human mediated dispersal.
592 More efficient means to detect and quantify (soil-borne) inoculum of *P. megakarya* will also go
593 a long way to help elucidate the factors that govern BPD epidemics in cacao. Based on our observations
594 some infection cluster appeared and disappeared over time thus we believe there is a steady influx of
595 exogenous inoculum throughout the years. Yet in the observed plantations, in spite of this steady influx,
596 *P. megakarya* seemed to have difficulty establishing itself. This seems to be somewhat contradictory in
597 light of the multiple possibilities that *P. megakarya* has to survive in cacao plantations. *Phytophthora*
598 *megakarya* can survive up to 18 months in the soil (Ward and Griffin, 1981). Several intercropped
599 species (*Elaeis guineensis*, *Persea Americana*) and *Musa* spp. (present during the first 2-3 years after
600 plot installation in 2006) were identified as "alternative" hosts for *P. megakarya* (Akrofi *et al*., 2015)
601 yet here no contribution to BPD establishment and dispersal was observed. On the contrary, *C. nucifera*
602 and *E. guineensis* seem to act as a barrier in Bakoa as supported by a PSA mainly present within
603 columns. Moreover, claims that *P. megakarya* can survive and remain viable for many months in bark,
604 wood, and plant debris and readily cause cankers (Akrofi, 2015; Appiah *et al*., 2004) have to be
605 interpreted somewhat cautiously. Ali *et al* (2016) e.g. showed that out of a sample of 39 *Phytophthora*
606 isolates collected in Ghana between 1993 and 2012, identified as *P. megakarya*, 38 were actually *P.*
607 *palmivora*. Yet, the idea that *P. megakarya* survives elsewhere than the soil cannot be discarded either
608 given the high level of intra-tree dispersal, the significant link for within tree disease incidence between
609 subsequent years and low presence in the soil. The findings here do however, clearly indicate the
610 difficulty of *P. megakarya* establishment in the studied plots.
611 In summary, the results indicate that in new plantings primary inoculum plays a more important
612 role than previously thought in disease epidemics. That being so, more attention should be focused on
613 management of primary inoculum. By rigorous phytosanitation, as soon as first infections are observed,
614 disease progress over years can be slowed and the build-up of a soil inoculum reservoir limited. By
615 slowing the build-up of the inoculum reservoir, phytosanitation in young cacao plantations actually
616 seems to be more effective as a preventative measure compared with phytosanitation in plantations
617 where a substantial inoculum reservoir exists. Such a practice would reduce the need for fungicide
618 applications. However, this means altering the mind-set of farmers since they generally start
619 phytosanitation only when the disease surpasses a certain threshold, often providing the pathogen with
620 ample time to build an inoculum reservoir. Accompanying measures to further limit the establishment

of an inoculum reservoir such as e.g. soil applications with biocontrol agents could provide additional means to limit disease progression.

Since the disease had difficulty establishing itself in the studied plots, it was the surrounding environment that provided a steady source of exogenous inoculum. Consequently, efforts should be made to limit primary inoculum of *P. megakarya* arrival by maintaining sufficient distance or using other plant species as barriers when creating new cacao plantations. Such a strategy is also envisioned in Côte d'Ivoire and Ghana to limit the impact of CSSV disease and would thus have the added benefit of limiting BPD. Furthermore, as proven by the flooding event, flood prone areas should be avoided as rivers can transport *P. megakarya* propagules. Nonetheless, the presence of river near a cacao plantation could be beneficial for irrigation and serves as a water source for e.g. pesticide applications. This study is a first on how newly established cacao cropping systems become infected with *P. megakarya*. Complementary studies are needed for further clarification on the mechanisms for long range (> 6 m) dispersal, the identification of inoculum entry pathways and the processes and factors that govern within tree dispersal in order to improve management strategies of BPD.

Acknowledgements

The authors gratefully acknowledge funding by CIRAD through ATP Omega3, ATP Safsé, and the 'Dispositif en partenariat (DP)' Agroforesterie Cameroun. We would like to thank CIRAD and IRAD staff that helped implement the project and provided useful information. We especially thank Olivier Sounigo, Raymond Bourgoing, Bruno Efombagn, Zacharie Techou, Sandrine Petchayo and Christian Nembot for their participation. We also address our gratitude to the farmers Emile Ohono, Robert Kanigoule†, Andre Belebele and Germain Bilongo who agreed to work with us on their farms.

643 **References**

644 Akrofi, A. Y. 2015. *Phytophthora megakarya*: a review on its status as a pathogen on cacao in West
645 Africa. *Afr. Crop. Sci*. 23:67-87.

646 Akrofi, A. Y., Amoako-Atta, I., Assuah, M., and Asare, E. K. 2015. Black pod disease on cacao
647 (*Theobroma cacao* L) in Ghana: spread of *Phytophthora megakarya* and role of economic plants
648 in disease epidemiology. *Crop Prot.* 72:66-75.

649 Agresti, A. 2007. An Introduction to Categorical Data Analysis, 2nd ed John Wiley & Sons394p.

650 Ali, S. S., Amoako-Atta, I., Bailey, R. A., Strem, M. D., Schmidt, M., Akrofi, A. Y., Surujdeo-Maharaj,
651 S., Kolawole, O. O., Begoude, D. B. A., ten Hoopen, G. M., Goss, E., Mora, P. W., Meinhardt,
652 and Bailey, A. B. 2016. PCR-based identification of cacao black pod causal agents and
653 identification factors possibly contributing to *Phytophthora megakarya's* field dominance in
654 West Africa. *Plant pathol.* 65:1095-1108 doi: 10.1111/ppa12496.

655 Appiah. A. A., Opoku. I. Y., and Akrofi. A. Y. 2004. Natural occurrence and distribution of stem cankers
656 caused by *Phytophthora megakarya* and *Phytophthora palmivora* on cocoa. *Eur. J. Plant*
657 *Pathol*. 110: 983-990

658 Bailey, B.A., Ali, S., Akrofi, A.Y., and Meinhardt, L. 2016. *Phytophthora megakarya*, a causal agent of
659 black pod rot in Africa. In Cacao diseases: a history of old enemies and new encounters. Eds.
660 Bailey B.A. &. Meinhardt L.W., pp. 267-303. *Springer* 630pp.

661 Barzman, M., Bàrberi, P., Birch, A. N. E., Boonekamp, P., Dachbrodt-Saaydeh, S., Graf, B., Hommel,
662 B., Jensen, J. E., Kiss, J., Kudsk P., Lamichhane, J. R., Messéan, A., Moonen, A. C., Ratnadass,
663 A., Ricci, P., Sarah, J. L., and Sattin, M. 2015. Eight principles of integrated pest management.
664 *Agron. Sustain. Develop.* 35:1199-1215 doi: 10 007/913593-015-0327-9.

665 Beilhe, B. L., Ketchiemo, T. F., and Niemenak, N. 2017. Analyse de la relation dégâts dommages entre
666 mirides et cacaoyer. *Int. Cacao Res. Symp.* 2017-11-13/2017-11-17, Lima, Peru.

667 Besag, J. 1977. Contribution to the discussion of Dr Ripley's paper. *J. Roy. Stat. Soc.* B39:193-195.

668 Bonnot, F., de Franqueville, H., and Lourenço, E. 2010. Spatial and spatiotemporal pattern analysis of
669 coconut lethal yellowing in Mozambique. *Phytopathology* 100:300-312.

670 Brasier, C. M., and Griffin, M. J. 1979. Taxonomy of *Phytophthora palmivora* on cacao. Transactions
671 of the *Br. Mycol. Soc.* 72(1):111-143.

672 Brasier, C. M., Griffin, M. J., Ward, M. R., Idowu, O. L., Taylor, B., and Adedoyin. S. F. 1981.
673 Epidemiology of *Phytophthora* on Cocoa in Nigeria: No. 25. Final Report of the International
674 Cocoa Black Pod Research Project. *Commonw. Mycol. Inst. Kew. Phytopathol. Pap*. Kew,
675 Surrey-London; 1981.

676 Bullock, J. M., Shea, K., and Skarpaas, O. 2006. Measuring plant dispersal: an introduction to field
677 methods and experimental design. *Plant Ecol.* 186:217–234.

678 Butler, D. R. 1980. Dew and Thermal lag: measurements and an estimate of wetness duration on cacao
679 pods. *Quart. J. Met. Soc.* 106: 539-550.
680 Campbell, C. L., and Madden, L. V. 1990. Spatial aspects of plant disease epidemics II: analysis of
681 spatial patterns. In *Introduction to Plant Disease Epidemiology*, eds. CL Campbell and LV
682 Madden, 1:289–328. New York: Wiley. 532 pp.
683 Cliff, A. D., and Ord, J. K. 1981. Spatial processes: Models and applications. London, 266p.
684 Cressie, N. A. C. 1993. Statistics for Spatial Data. London, UK: Wiley–Blackwell.
685 Dakwa, J. T. 1987. A serious outbreak of black pod disease in a marginal area of Ghana. Proceedings
686 of the *10th Int. Cacao Res. Conf*., Santo Domingo, Dominican Republic, 17- 23rd May, 1987.
687 Dale, M. R. 1999. Concepts of spatial pattern analysis in plant ecology, In Spatial Pattern Analysis in
688 Plant Ecology, ed. M. Dale, pp. 1–30. *Cambridge. Univ. Press.* 326 pp.
689 Deberdt, P., Mfegue, C. V., Tondje, P. R., Bon, M. C., Ducamp, M., Hurard, C., Begoude, B. A. D.,
690 Ndoumbe-Nkeng, M., Hebbar, P. K., and Cilas, C. 2008. Impact of environmental factors,
691 chemical fongicide and biological control on cacao pod production dynamics and black pod
692 disease (*Phytophthora megakarya*) in Cameroun. *Biol. Cont.* 44:149-159.
693 Djiekpor, E. K., Partiot, M., and Lucas, P. 1982. The cacao black pod disease due to *Phytophthora* sp
694 in Togo determination of species responsible. *Cafe Cacao Thé* 26 (2):97-108.*
695 European Union, 2009. Directive 2009/128/EC of the European parliament and of the council of 21
696 October 2009: establishing a framework for Community action to achieve the sustainable use
697 of pesticides. *Official journal of the European Journal* 309/71.
698 Evans, H. C., 1973. Invertebrate vectors of *Phytophthora palmivora* causing black pod disease of cocoa
699 in Ghana. *Ann. Appl. Biol*., 75: 331-345.
700 Fay P. M., Hunsberger, A S., Nason, M., and Gabriel, E. 2018. Exact Tests and Confidence Intervals for
701 2x2 Tables. R package version 1.6.3, p25.
702 Flood, J., Guest, D., Holmes, K.A., Keane, P., Padi, B., and Sulistyowati, E. 2004. Cocoa under attack.
703 In: J. Flood & R. Murphy (Eds.), Cocoa futures (p. 164). Chincina, CO: CABIFEDERACAFE.
704 Gidoin, C., Babin, R., Beilhe, L. B., Cilas, C., Hoopen, G. M. T., and Bieng, M. A. N. 2014. Tree spatial
705 structure, host composition and resource availability influence mirid density or black pod
706 prevalence in cacao agroforests in Cameroon. *PLoS ONE*, 9 (10) e109405 doi:10.1371.
707 Goreaud, F. 2000. Apports de l'analyse de la structure spatiale en forêt tempérée à l'étude et à la
708 modélisation des peuplements complexes. Thèse de doctorat, *ENGREF*, centre de Nancy,
709 France, p 526.
710 Gregory, P. H. 1974. *Phytophthora* disease of cacao. *Longman Group Limited*, London, 348p.
711 Gregory, P., Griffin, M., Maddison, A., and Ward, M. 1984. Cocoa black pod: A reinterpretation. *Cocoa*
712 *Growers' Bulletin* 35, 5-22.
713 Gregory, P. H., and Maddison, A. C. 1981. Epidemiology of *Phytophthora* on Cocoa in Nigeria.
714 *Commonw. Mycol. Inst. Kew. Phytopathol. Pap*. No. 25.

715 Guest, D. 2007. Black pod: diverse pathogens with a global impact on cacao yield. *Phytopathology.*
716 97:1650–1653.
717 Holmes, K. A., Evans, H. C., Wayne, S., and Smith, J. 2003. *Irvingia*, a forest host of the cacao black
718 pod pathogen, *Phytophthora megakarya*, in Cameroon. *Plant Pathol.* 52:486–490
719 International Cocoa Organization, 2014. Economics Committee: The cocoa market situation. *4th*
720 *meeting*, London, 16-18 September 2014.
721 Jagoret, P., Michel-Dounias, I., Snoeck, D., Todem Ngnogué, and H., Malezieux E. 2012. Afforestation
722 of savannah with cacao agroforestry systems: a small-farmer innovation in central Cameroon.
723 *Agrofor. Syst.* 86:493–50.
724 Jolles, E. A., Sullivan, P., Alker, P. A., and Harvell, D. C. 2002. Disease transmission of aspergillosis
725 in sea fans: inferring process from spatial pattern. *Ecology*, 83(9), 2373–2378.
726 Jung, T., Blaschke, M. 2004. Phytophthora root and collar rot of alders in Bavaria: Distribution, modes
727 of spread and possible management strategies. *Plant Pathol*. 53: 197– 208.
728 Landcaster J., and Downes, B. J., 2004. Spatial point pattern analysis of available and exploited
729 resources. *Ecography*, 27:94-102.
730 Koenig, W.D. 1999. Spatial autocorrelation of ecological phenomena. *Tree* 14:22-26
731 Konam, J. K., & Guest, D. I. 2004. Role of beetles (Coleoptera: Scolytidae and Nitidulidae) in the spread
732 of *Phytophthora palmivora* pod rot of cocoa in Papua New Guinea. *Australas. Pl. Pathol*. 33:55–
733 59.
734 Maddison, A. C., and Griffin, M. J. 1981. Detection and movement of inoculum. In: Gregory, P. H. &
735 Maddison A. C. (Eds.), Epidemiology of *Phytophthora* on cocoa in Nigeria, *Commonw. Mycol.*
736 *Inst. Kew. Phytopathol. Pap*. No. 25.
737 Mahob, R. J., Baleba, L., Yede, Dibog, L., Cilas, C., Bilong Bilong, C. F., and Babin, R. 2015. Spatial
738 distribution of *Sahlbergella singularis* hagl. (hemiptera: miridae) populations and their damage
739 in unshaded young cacao-based agroforestry systems. *Int. J. Plant Animal Environ. Sci*. 5:121-
740 131 ISSN 2231-4490.
741 Malewski, T., Brzezińska, B., Belbahri, L., and Oszako, T. 2019 Role of avian vectors in the spread
742 of *Phytophthora* species in Poland. *Eur. J. Plant Pathol*. 155: 1363–1366.
743 Medeiros, A. G. 1967. Caracterizacao de area 'Foco' da 'podridao parda'. *Infome Technico* CEPEC, 38-
744 39.
745 Mfegue, V. 2012. Origine et mécanismes de dispersion des populations de *Phytophthora megakarya*,
746 pathogène du cacaoyer au Cameroun. Thèse de doctorat. *Centre international d'études*
747 *supérieures en sciences agronomiques* Montpellier-SupAgro, 186p
748 Monteith, L. J., and Butler, D. R. 1979. Dew and Thermal lag: a model for cocoa pods. *Quart. J. Met.*
749 *Soc.* 105:207-215.

Muller, E. 2016. Cacao Swollen Shoot Virus (CSSV): history, biology, and genome, In Cacao diseases: a history of old enemies and new encounters. Eds. Bailey B.A. &. Meinhardt L.W., pp. 337-358. *Springer* 630pp.

Nembot, C., Takam Soh, P., ten Hoopen, G.M., and Dumont, Y. 2018. Modeling the temporal evolution of cocoa black pod rot disease caused by *Phytophthora megakarya. Math Meth Appl Sci.* 41:8816–8843. DOI: 10.1002/mma.5206

Ndoumbè-Nkeng, M. 2002. Incidence des facteurs agro-écologiques sur l'épidémiologie de la pourriture brune des fruits du cacaoyer au Cameroun : contribution à la mise en place d'un modèle d'avertissements agricoles. Thèse de Doctorat. *Institut National Agronomique Paris-Grignon.*

Ndoumbè-Nkeng, M., Cilas, C., Nyemb, E., Nyasse, S., Flori, A., and Sache, I. 2004. Impact of removing disease pods on cacao black pod caused by *Phytophthora megakarya* and on cacao production in Cameroon. *Crop Prot.* 23 (5):415-424.

Ndoumbè-Nkeng, M., Efombagn, M. I. B., Nyasse, S., Nyemb, E., Sache, I. and Cilas, C. 2009. Relationships between cacao *Phytophthora* pod rot disease and climatic variables in Cameroon. *Plant Pathol.* 31: 309-320.

Ndoumbè-Nkeng, M., Efombagn, M. I. B., Bidzanga, N. L., Sache, I., and Cilas, C. 2017. Spatio-temporal dynamics on a plot scale of cacao black pod rot caused by *Phytophthora megakarya* in Cameroon. *Eur. J. Plant Pathol*. 147:579–590.

Ndoungué, M., Petchayo, S., Techou, Z., Nana, W. G., Nembot, C., Fontem, D., and Ten Hoopen, G. M. 2018. The impact of soil treatments on black pod rot (caused by *Phytophthora megakarya*) of cacao in Cameroon. *Bio. Cont.* 123:9-17.

Neher, D., and Duniway, J.M. 1992. Dispersion of *Phytophthora parasitica* in tomato fields by furrow irrigation. *Plant Dis*. 76: 582-586.

Ngo Bieng, M. A., Gidoin, C., Avelino, J., Cilas, C., Deheuvels, O., and Wery, J. 2013. Diversity and spatial clustering of shade trees affect cacao yield and pathogen pressure in Costa Rican agroforests, *Bas. App. Ecol.* 14(4):329–336.

Ngwohgi, M. F. 2015. Rôle des fourmis arboricoles dans la dissémination de *Phytophthora megakarya* Brasier et Griffin, agent causal de la pourriture brune du cacaoyer (*Theobroma cacao* L.) au Cameroun. *Mémoire de Master, Université de Yaoundé I*, 71p.

Nyasse, S., Grivet, L., Risterucci, A. M., Blaha, G., Berry, D., and Lanaud, C. 1999. Diversity of *Phytophthora megakarya* in Central and West Africa revealed by isozyme and RAPD markers. *Mycol. Res.* 103:1225- 1234.

Nyassé S., Efombagn M.I.B., Kébé B.I., Tahi G.M., Despréaux D., Cilas C. 2007. Integrated management of Phytophthora diseases on cocoa (*Theobroma cacao* L.): impact of plant breeding on pod rot incidence. *Crop Prot.* 26: 40-45.

Opoku, I. Y., Akrofi, A. Y. and Appiah, A. A. 2002. Shade trees are alternative hosts of the cacao pathogen *Phytophthora megakarya*. *Crop Prot.* 21:629-634.

787 Opoku, I. Y., Assuah, M. K., and Aneani, F. 2007. Management of black pod disease of cacao with
788 reduced number of fungicide application and crop sanitation. *Afr. J. Agri. Res.* 2:601-604.
789 Oro, Z. F., Bonnot, F., Ngo-Bieng, M. A., Delaitre, E., Dufour, P. B., Ametefe, E. K., Mississo, E.,
790 Wegbe, K., Muller, E., and Cilas, C. 2012. Spatiotemporal pattern analysis of cacao swollen
791 shoot virus in experimental plots in Togo. *Plant Pathol.* 61:1043–1051.
792 Pélissier, R., and Goreaud, F. 2015. Ads: Spatial point patterns analysis. R package version 1.5-2.2.
793 Pion. 266 p.
794 Ploetz, R. 2016. The impact of diseases on cacao production: a global overview, In Cacao diseases: a
795 history of old enemies and new encounters. Eds. Bailey B.A. &. Meinhardt L.W., pp. 33-59.
796 *Springer* 630pp.
797 Puig, A. S., Ali, S., Strem, M., Sicher, R., Gutierrez, O. A., and Bailey, B. A. 2018. The differential
798 influence of temperature on *Phytophthora megakarya* and *Phytophthora palmivora* pod lesion
799 expansion, mycelia growth, gene expression, and metabolite profiles. *Physiol. Mol. Plant*
800 *Pathol.* 102:95-112.
801 R Core Team, 2013. R: A language and environment for statistical computing. R Foundation for
802 Statistical Computing, Vienna, Austria.
803 Reynolds, K. M., and Madden, L. V. 1988. Analysis of epidemics using spatio-temporal autocorrelation.
804 *Phytopathology* 78:240-246.
805 Ristaino, J. B., and Gumpertz, M. L. 2000. New frontiers in the study of dispersal and spatial analysis
806 of epidemics caused by species in the genus *Phytophthora*. *Annu. Rev. Phytopathol*. 38:541-
807 576.
808 Risterucci, A. M., Paulin, D., Ducamp, M., N'Goran, J. A. K., and Lanaud, C. 2003. Identification of
809 QTLs related to cacao resistance to three species of *Phytophthora*. *Theor. Appl.Genet.*108:168-
810 174
811 Sansome, E., Brasier, C. M., and Griffin, M. J. 1975. Chromosome size differences in *Phytophthora*
812 *palmivora*, a pathogen of cacao. *Nature* 255:704-705.
813 Sansome, E., Brasier, C. M., and Sansome, F. W. 1979. Further cytological studies on the 'L' and 'S'
814 types of *Phytophthora* from cacao. *Trans. Br. Mycol. Soc.* 73(2):293-302.
815 Solla, A, and Camarero J. J., 2006 Spatial patterns and environmental factors affecting the presence of
816 *Melampsorella caryophyllacearum* infections in an *Abies alba* forest in NE Spain. *Forest*
817 *Pathology* 36:165 - 175
818 Ten Hoopen, G. M., Sounigo O., Babin, R., Yédé, Dikwe, G., and Cilas, C. 2010. Spatial and temporal
819 analysis of a *Phytophthora megakarya* epidemic in a plantation in the Centre of Cameroon. *16th*
820 *Int. Cacao Res. Conf.* 2009-11-16/2009-11-21, Bali, Indonésie.
821 Themann, K., Werres, S., Luttmann, R., and Diener, H. A. 2002. Observations of *Phytophthora* spp. in
822 water recirculation systems in commercial hardy ornamental nursery stocks. *Eur. J. Plant*
823 *Pathol.* 108:337-343.

824 Tjosvold S. A., Chambers D. L., Davidson J. M. and Rizzo D. M., 2002. Incidence of *Phytophthora*
825 *ramorum* inoculum found in soil collected from a hiking trail and hikers' shoes in a California
826 Park. In Proceedings of Sudden Oak Death, a Science Symposium, USDA Forest Service and
827 University of California, Berkeley 53p.
828 Ward, M. R., and Griffin, M. J. 1981. Soil phase of cacao *Phytophthora*. In: Epidemiology of cacao in
829 Nigeria. Gregory, P. H. (ed.) Common. *Mycol. Inst. Phytopathol*. *Pap*. 25:50-61.
830

831 Table 1: Odds ratio, lower limit of confidence interval (inf. CI) and P-value of one-sided Fisher exact
832 test for three hypotheses about the relationship between disease incidence and soil infections of *P.*
833 *megakarya* in cacao.

Transition year	Odds ratio	Inf. CI	P-value
H1:Disease incidence in year *t* related to soil infection in year *t+1*			
2013-2014	0.44	0.20	0.043
2014-2015	0.38	0.16	0.015
2015-2016	0.54	0.24	0.133
H2: Disease incidence in year *t* related to disease incidence in year *t+1*			
2013-2014	3.34	2.22	<0.001
2014-2015	3.11	1.90	<0.001
2015-2016	5.46	3.07	<0.001
H3: Soil infection in year *t* related to soil infection in year *t+1*.			
2013-2014	2.30	0.42	0.364
2014-2015	1.79	0.46	0.465
2015-2016	13.77	4.36	<0.001

834

835

836

837 Table 2: Odds ratio, lower limit of confidence interval (inf. CI) and P-value of one-sided Fisher exact
838 test for three hypotheses about the relationship between primary and secondary infections of *P.*
839 *megakarya* in cacao

Year/Transition year	Odds ratio	Inf. CI	P-value
H4: More secondary infections in year *t* derive from primary infections in year *t*			
2011	239.19	101.02	<0.001
2013	194.23	98.80	<0.001
2014	23.81	16.58	<0.001
2015	374.73	168.91	<0.001
2016	83.34	47.98	<0.001
H5: Higher number of infected trees in year *t* leads to higher number of primary infections in year t_{+1}			
2013-2014	3.75	2.52	<0.001
2014-2015	4.65	2.98	<0.001
2015-2016	7.37	4.26	<0.001
H6: More secondary infections in year *t* generate more primary infections in year t_{+1}.			
2013-2014	4.02	2.68	<0.001
2014-2015	4.38	2.71	<0.001
2015-2016	6.28	3.30	<0.001

840

841

842 Table 3: Mean maximum temperature ($T_{max,}$ °C), mean daily temperature amplitude (T_{ampl}, °C), mean
843 time per day T> 30°C ($T_{>30°C,}$ hour.day^{-1}), Mean Minimum relative humidity (RH_{min}, %) and mean daily
844 RH amplitude (RH_{ampl}, %) for each plot in different locations

Plot	ID loggers	T_{max} °C *	T_{ampl} °C	T>30°C	RH_{min} %	RH_{ampl} %
Bakoa[1]	B1	32.3b	11.0ab	4.0ab	63.8ab	40.6c
	B2	31.4ab	10.0ab	3.5ab	66.3b	34.1b
	B4	33.4b	12.4b	4.5b	62.8ab	37.2b
	B5	33.0b	11.7ab	3.9ab	60.4ab	39.6c
	B6	29.8a	8.8a	3.0a	70.1b	35.3b
	B7	29.8a	8.6a	2.6a	40.8a	59.2d
	B8	31.8ab	10.7ab	3.9ab	63.1ab	36.8b
	B9	29.6a	8.7a	3.1a	68.5b	31.5b
	B10	34.7c	13.6b	4.9b	54.9ab	44.5c
	B11	31.3ab	9.1a	3.7ab	84.1c	14.9a
	B12	33.1b	12.1b	3.8ab	38.3a	61.6d
	B13	32.4b	11.3ab	4.1ab	62.5ab	38.0b
Kédia	K1	35.9c	15.2c	5.5ab	55.5c	43.6ab
	K2	33.7b	13.2b	7.6b	46.3b	53.7b
	K3	34.2bc	13.9b	5.1ab	47.6b	52.0b
	K4	31.8a	11.6a	3.5a	63.0d	37.6a
	K5	35.9c	15.6c	4.9ab	39.9a	59.8c
	K6	34.8bc	14.5bc	5.2ab	59.0c	40.9a
Ngat	N1	26.5a	6.95a	0.0a	68.7bc	29.9b
	N4	28.7b	8.61b	2.0b	71.6c	28.2ab
	N5	29.9bc	10.48c	1.9b	50.4a	49.6c
	N6	29.7bc	10.19c	2.0b	68.8bc	31.0b
	N7	29.9bc	10.21c	2.3b	57.6a	42.3c
	N8	31.6c	11.63d	2.6b	63.5b	36.7bc
	N9	29.5bc	10.03c	1.8b	76.3c	23.7a
Mean Bakoa**	-	31.9y	10.6y	3.8y	61.4y	39.4y
Mean Kédia	-	34.4z	14.0z	4.7z	51.9x	47.9z
Mean Ngat	-	29x	9.3x	1.8x	66.4z	32.8x

845 *Values in the same column followed by the same letter are not statistically different from other values
846 in the same plot (Kruskal-Wallis and Wilcoxon rank test at P=0.05).
847 **Mean values per plot, values in the same column followed by the same letter are not statistically
848 different between plots (Kruskal-Wallis and Wilcoxon rank test at P=0.05).

Figure legends

Figure 1: Plot layouts and their neighbouring environments as established in 2009 and locations of Tinytag temperature and relative humidity data loggers in 2016 (black squares) (top of the figures). Subsequent plot layouts show the spatial distribution of the three cacao health statuses starting from the year first infections were observed for Bakoa, from 2011 to 2016, where cacao is interspersed with lanes containing oil palm (to the left) and coconut (to the right), Kédia, from 2010 to 2016, where cacao is interspersed with oil palm trees and Ngat, from 2009 to 2016, where certain cacao trees are replaced with fruit trees (f). Slope direction is indicated from top to bottom by the arrow on the right. The orange line in Ngat scheme, marks a well traversed footpath.

Legend: each square corresponds to a cacao tree with as status either "Healthy" (grey), "Infected" (black), or "Non-Productive" (light grey). White areas correspond to areas where no cacao was grown either because of the interspersed oil palm (Bakoa and Kédia), coconut (Bakoa) or fruit trees (Ngat NGA) or because of the presence of other crops. Locations with a horizontal bar depict soil sample locations testing negative, and triangles depict soil sample locations testing positive for the presence of *P. megakarya.*

Figure 2: Ripley function L(r) for "Infected" cacao trees for Bakoa from 2013 to 2016, Kédia from 2011 to 2016 and Ngat from 2011 to 2016.

Solid line = observed values; dashed lines = 0.99 confidence interval under the hypothesis of complete spatial randomness obtained through simulation of 10 000 L(r) curves using the Monte Carlo method.

Figure 3: Correlograms showing the results (in p-values) of the join count statistics analysis between "Infected" cacao trees for Bakoa from 2010-2016, Kédia from 2011-2016 and Ngat from 2009 to 2016. Correlograms are symmetrical with respect to the origin.

Figure 4: Total number of infected cacao trees per year, per plot.

Figure 5: Temporal dynamics of primary and secondary infections over time in Bakoa from 2010-2016, Kédia from 2011-2016 and Ngat from 2011-2016. For all plots year 2012 is absent since data is incomplete for this year.

Solid line= primary infections, dashed line= secondary infections

Horizontal lines at the top of the graph depict the dry - - - - - and the wet —··—·· seasons.

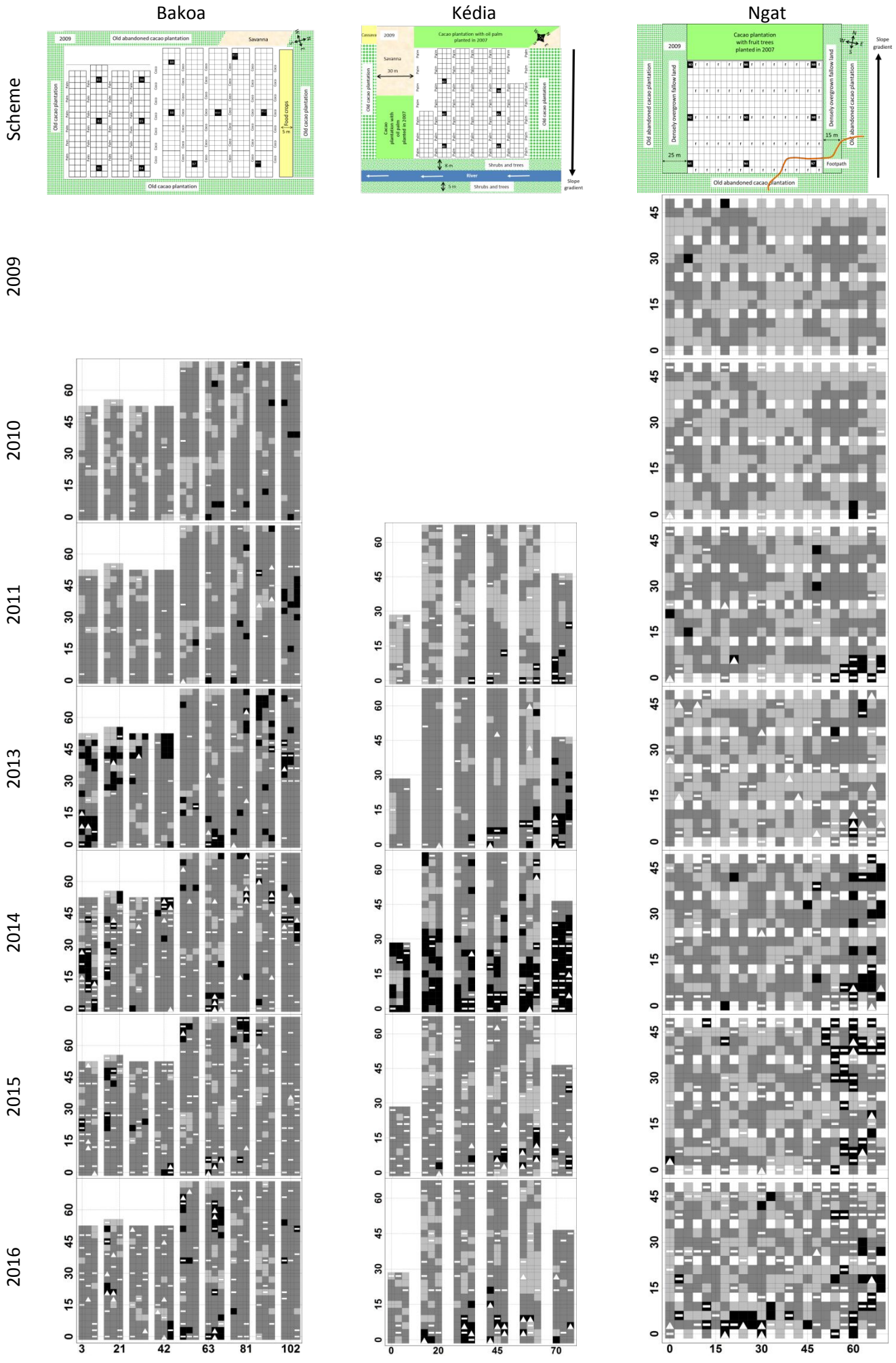
Bakoa
Kédia
Ngat
Scheme
2009
2010
2011
2013
2014
2015
2016
Old abandoned cacao plantation
Savanna
Old cacao plantation
Food crops
Cacao plantation with oil palm planted in 2007
Cassava
Shrubs and trees
River
Slope gradient
Cacao plantation with fruit trees planted in 2007
Densely overgrown fallow land
Footpath
3 21 42 63 81 102
0 20 45 70
0 15 30 45 60

Figure 1: Plot layouts and their neighbouring environments as established in 2009 and locations of Tinytag temperature and relative humidity data loggers in 2016 (black squares) (top of the figures). Subsequent plot layouts show the spatial distribution of the three cacao health statuses starting from the year first infections were observed for Bakoa, from 2011 to 2016, where cacao is interspersed with lanes containing oil palm (to the left) and coconut (to the right), Kédia, from 2010 to 2016, where cacao is interspersed with oil palm trees and Ngat, from 2009 to 2016, where certain cacao trees are replaced with fruit trees (f). Slope direction is indicated from top to bottom by the arrow on the right. The orange line in Ngat scheme, marks a well traversed footpath.

Legend: each square corresponds to a cacao tree with as status either “Healthy” (grey), “Infected” (black), or “Non-Productive” (light grey). White areas correspond to areas where no cacao was grown either because of the interspersed oil palm (Bakoa and Kédia), coconut (Bakoa) or fruit trees (Ngat) or because of the presence of other crops. Locations with a horizontal bar depict soil sample locations testing negative, and triangles depict soil sample locations testing positive for the presence of *P. megakarya.*

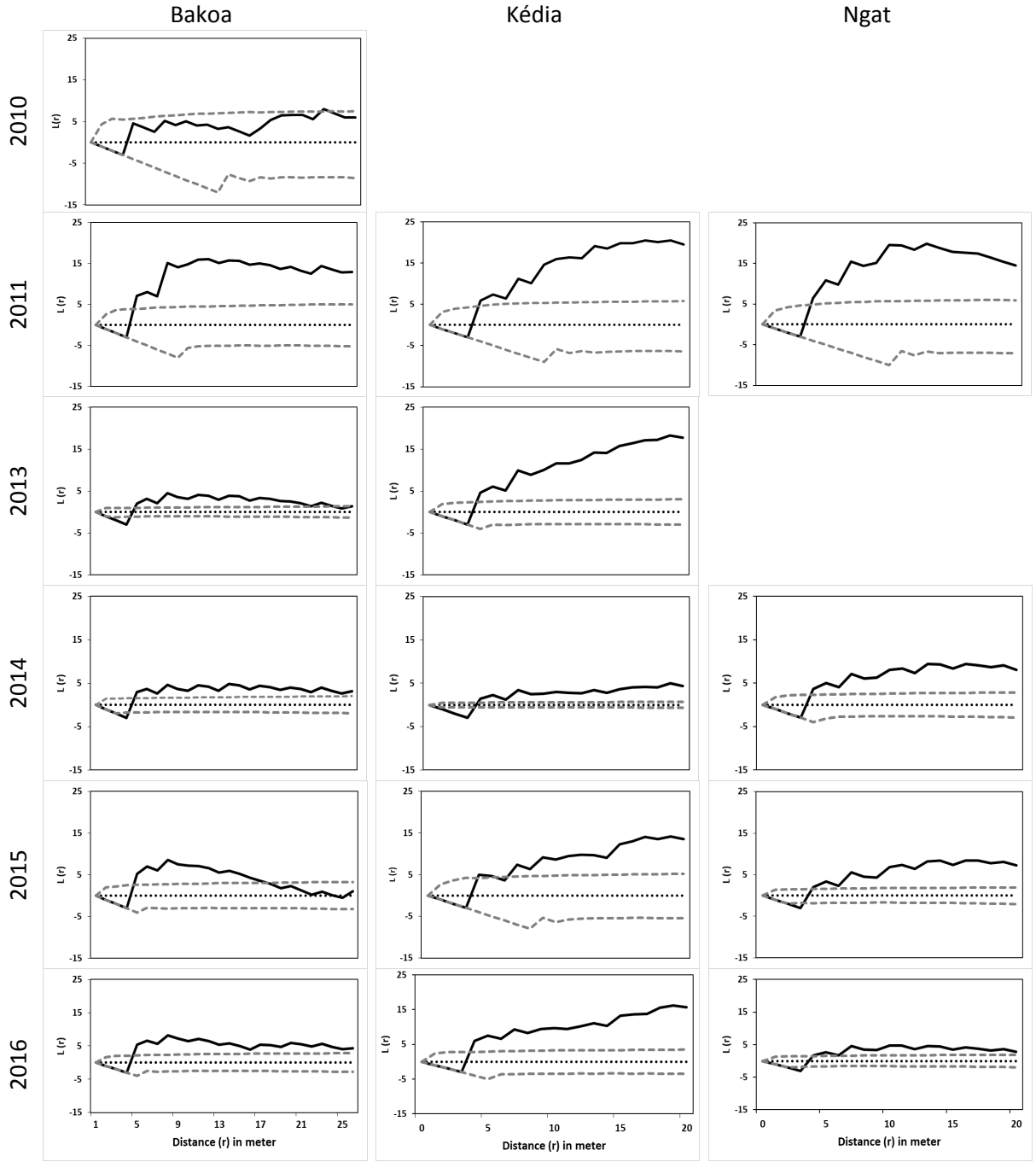

Figure 2: Ripley function L(r) for "Infected" cacao trees for Bakoa from 2013 to 2016, Kédia from 2011 to 2016 and Ngat from 2011 to 2016.

Solid line = observed values; dashed lines = 0.99 confidence interval under the hypothesis of complete spatial randomness obtained through simulation of 10 000 L(r) curves using the Monte Carlo method.

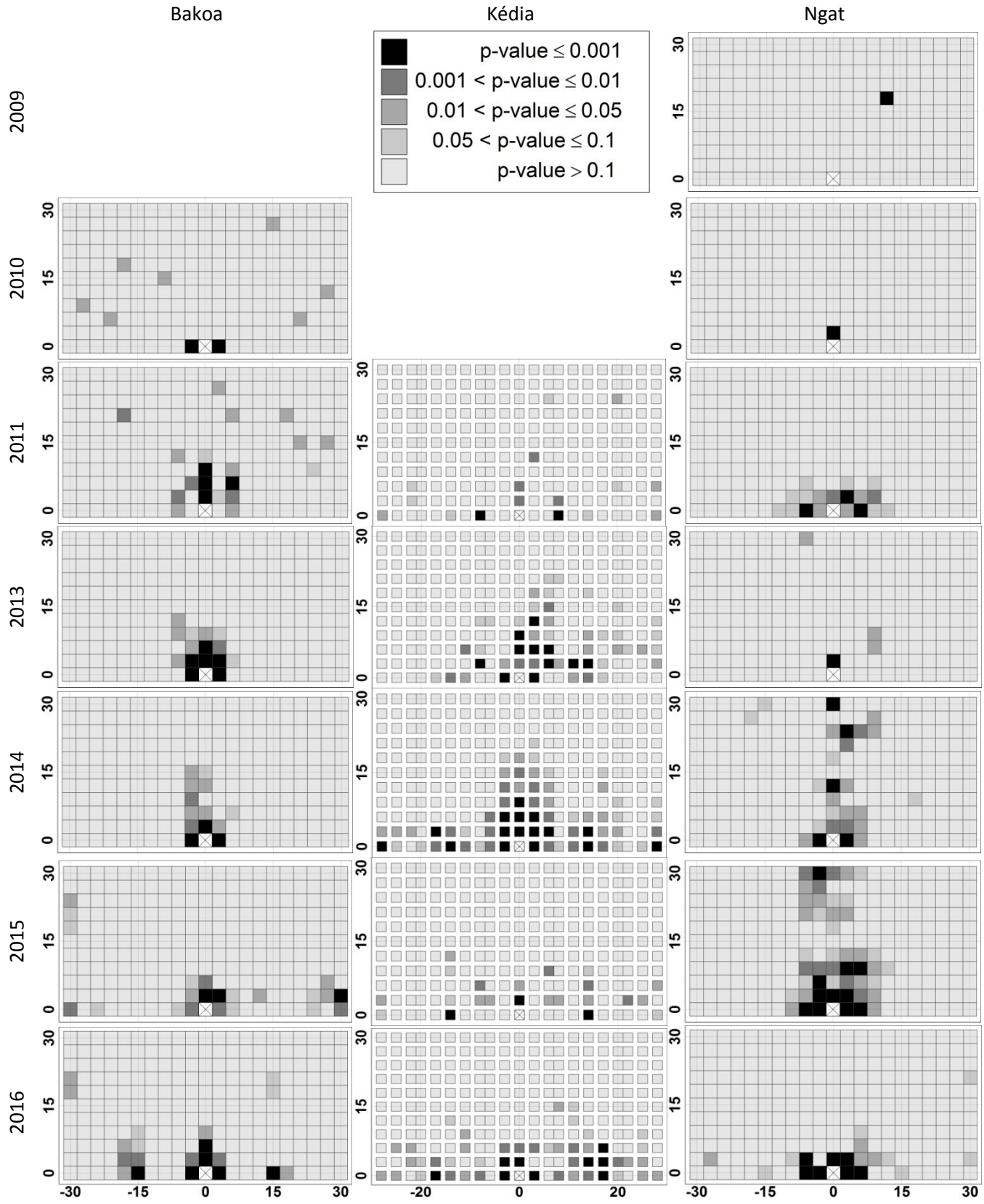

Figure 3: Correlograms showing the results (in p-values) of the join count statistics analysis between "Infected" cacao trees for Bakoa from 2010-2016, Kédia from 2011-2016 and Ngat from 2009 to 2016. Correlograms are symmetrical with respect to the origin.

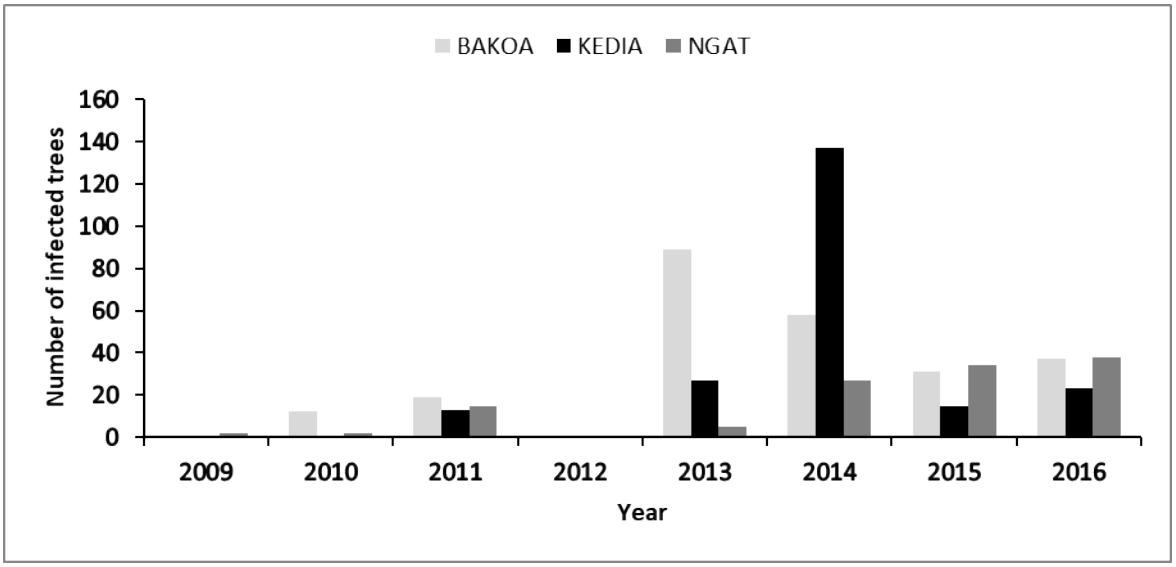

Figure 4: Total number of infected cacao trees per year, per plot.

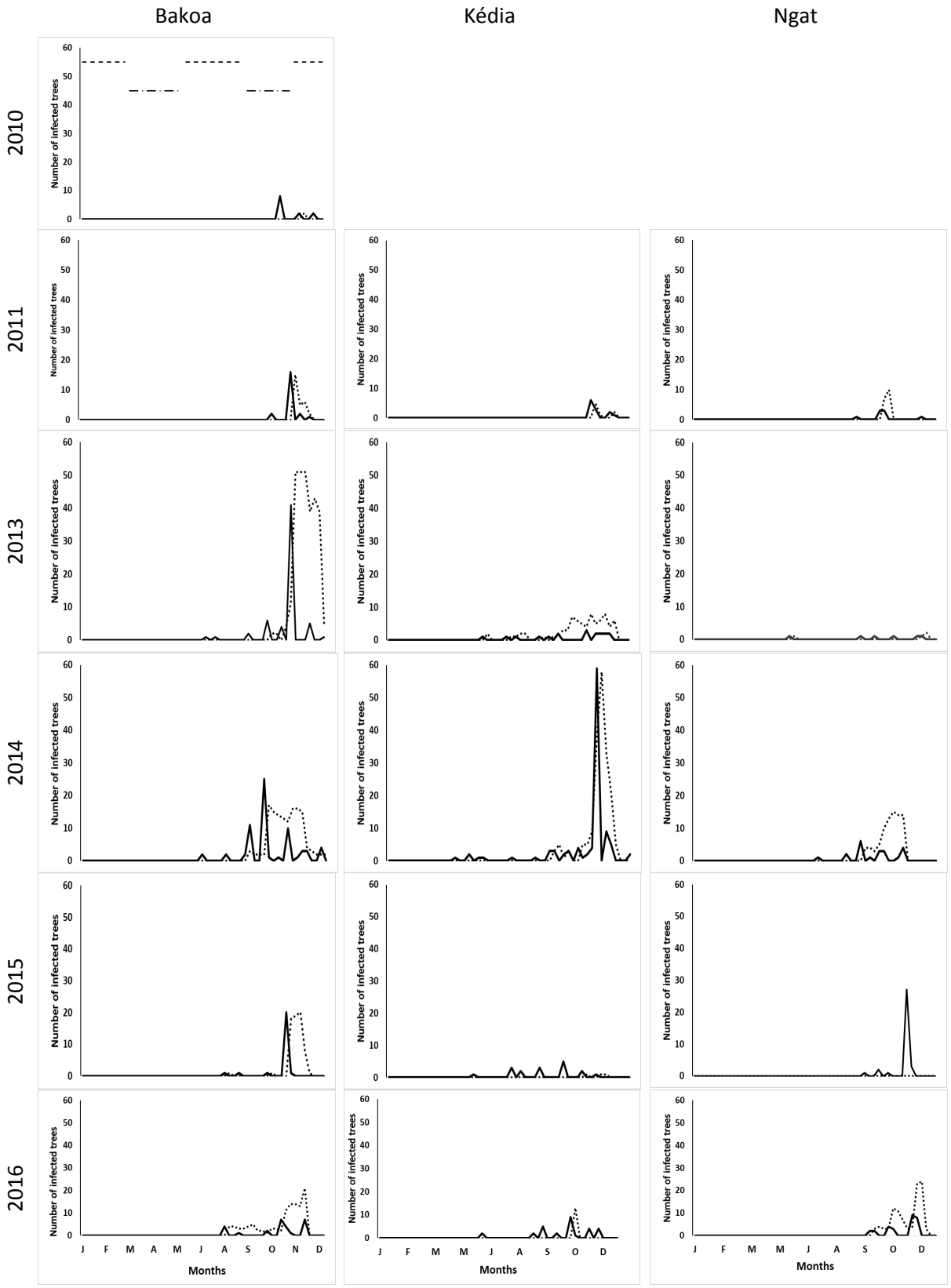
Bakoa
Kédia
Ngat
2010
2011
2013
2014
2015
2016
Number of infected trees
0
10
20
30
40
50
60
J F M A M J A S O N D
J F M M J A S O D
J F M M J A S O D
Months

Figure 5: Temporal dynamics of primary and secondary infections over time in Bakoa from 2010-2016, Kédia from 2011-2016 and Ngat from 2011-2016. For all plots year 2012 is absent since data is incomplete for this year.

Solid line= primary infections, dashed line= secondary infections

Horizontal lines at the top of the graph depict the dry - - - - - and the wet —·—·— seasons.

Table *e*-Xtra 1: List of planting materials present in the three smallholder cocoa plots

Type of planting material	Bakoa	Kédia	Ngat
Full-sibs from crosses	T 79/501 × SNK 413 PA 107 × M A12 UPA 143 × SNK 413 SNK 619 × GU 255/V SNK 608 × PA 70 UPA 143 × SNK 64 AMAZ 15/15 × SNK 413 T 79/501 × SNK 64 T 60/887 × SNK 64 IMC 67 × SNK 64 SCA 12 × SNK 16+REC T 79/501 × SNK 109 UPA 143 × SNK 64	IMC67 × SNK109 IMC 67 × SNK 64 SCA12 × SNK 16+REC T 79/501 × SNK 64 UPA 143 × SNK 64 PA 107 × SNK 614	IMC 67 × SNK 109 IMC 67 × SNK 64 SNK 109 × T 79/501 T 79/501 × SNK 109 UPA 143 × SNK 64 PA 107 × MO 20 SNK 625 × NA 33 BBK 1418 × MO 20
Clonal material	ICS 84 P 7 SNK 10 SNK 413		
Farmer selections	BK 1 BK 2 BK 3 BK 4 BK6 BK 7 BK 10 BK 12 TALBA 1 BK 3 BK 17		

Table *e*-Xtra 2: Number of soil samples per plot (Bakoa, Kédia, Ngat) and per year (2009 to 2016 except 2012) and the number and percentage of samples that tested positive for the presence of *P. megakarya,* for samples taken at the foot of trees classed either as “Healthy” or “Infected” the year before (except 2009).

		Number of soil samples			Number of soil samples positive for *P. megakarya**			Percentage soil samples positive for *P. megakarya*		
Plot	Year	Healthy trees	Infected trees	Total trees	Healthy trees	Infected trees	Total	Healthy trees	Infected trees	Total
	2009	20	0	20	0	-	0	0	-	0
	2010	40	0	40	2	-	2	5.0	-	5.0
	2011	47	8	55	2	0	2	4.3	0	3.6
Bakoa	2013	57	48	105	1	11	12	1.8 a	22.9 b	11.4
	2014	54	133	187	2	30	32	3.7 a	22.6 b	17.1
	2015	113	67	180	1	13	14	0.9 a	19.4 b	7.8
	2016	124	19	143	12	9	21	9.7 a	47.4 b	14.7
	2009	10	0	10	0	-	0	0	-	0
	2010	20	0	20	0	-	0	0	-	0
	2011	20	0	20	0	-	0	0	-	0
Kédia	2013	28	21	49	3	6	9	10.7 a	28.6 b	18.4
	2014	35	42	77	0	6	6	0 a	14.3 b	7.8
	2015	55	70	125	2	9	11	3.6 a	12.9 b	8.8
	2016	63	20	83	6	14	20	9.5 a	70.0 b	24.1
	2009	10	0	10	0	-	0	0	-	0
	2010	18	4	22	2	0	2	11.1	0	9.1
	2011	22	4	26	1	1	2	4.6	25.0	7.7
Ngat	2013	40	24	64	10	6	16	25.0 a	25.0 a	25.0
	2014	43	15	58	1	4	5	2.3 a	26.7 b	8.6
	2015	46	49	95	3	5	8	6.5 a	10.2 a	8.4
	2016	58	32	90	5	6	11	8.6 a	18.8 a	12.2
Total		923	556	1479	53	120	173	5.7 a	21.6 b	11.7

* Numbers in a row followed by the same letter do not differ at P=0.05 Fisher exact test